

Noisy Image Edge Detection Using an Uninorm Fuzzy Morphological Gradient

Manuel González-Hidalgo
 Computer Graphics and Vision Group.
 Maths. and Computer Science Dept.
 University of the Balearic Islands. Spain
 Email: manuel.gonzalez@uib.es

Arnau Mir Torres, Joan Torrens Sastre
 Fuzzy Logic and Information Fusion Group.
 Maths. and Computer Science Dept.
 University of the Balearic Islands. Spain
 Email: arnau.mir@uib.es, dmijts0@uib.es

Abstract—Medical images edge detection is one of the most important pre-processing steps in medical image segmentation and 3D reconstruction. In this paper, an edge detection algorithm using an uninorm-based fuzzy morphology is proposed. It is shown that this algorithm is robust when it is applied to different types of noisy images. It improves the results of other well-known algorithms including classical algorithms of edge detection, as well as fuzzy-morphology based ones using the Łukasiewicz t-norm and umbra approach. It detects detailed edge features and thin edges of medical images corrupted by impulse or gaussian noise. Moreover, some different objective measures have been used to evaluate the filtered results obtaining for our approach better values than for other approaches.

Keywords—Mathematical morphology, edge detection, noise reduction, representable uninorms, idempotent uninorm.

I. INTRODUCTION

Edge detection is a fundamental pre-processing step in applications such as image segmentation and computer vision, and its performance is relevant for the final results of the image processing. Over years, many efforts have been devoted in the literature, and also are currently devoted, to propose approaches to extract contour features. These different approaches vary from the classical approaches [1] based on a set of convolution masks, to the new techniques based on fuzzy sets [2]. Nevertheless, many of them fail or diminish their effectiveness in presence of noise.

The fuzzy mathematical morphology is a generalization of binary morphology [3] using techniques of fuzzy sets [4], [5], [6], [7]. Mathematical morphology, either crisp or fuzzy, provides an alternative approach to image processing based on the shape concept represented by the so called structural element (see for instance [3]). The fuzzy operators used to build a fuzzy morphology are conjunctors (usually t-norms) and implications. Recently conjunctive uninorms, as a particular case of conjunctors, have also been used in this area [8], [9], [10], [11]. More techniques for edge detection have been designed based on residuals and morphological gradients obtained from the crisp or fuzzy mathematical morphology. See by example, [11], [10] and references therein, [12], [13], and also [14] where morphological gradients were used to detect edges in CT medical images altered by noise.

All these works show that the morphological gradients remain relevant and useful in the analysis and image processing. In this work the feasibility of alternate filters will be studied, from opening and closing of the fuzzy morphology based on uninorms (studied in detail in [11]). Following the ideas in [10], where the authors used the alternate filters in the reduction of noise, we will use them in the design of an edge detection algorithm for medical images reaching a compromise between elimination and smoothing of noise and the detection of the features in medical images. A preliminary work in this direction is [9] where the proposed algorithm was already introduced. In this work, we study the performance of this algorithm in presence of different types of noise, impulse and Gaussian. Moreover, the behaviour of this algorithm is investigated depending on the amount of noise in the images. Some different objective measures are used to evaluate the filtered results, the Mean Square Error (MSE) and the Signal to Noise Ratio (SNR) (see [1]), and the recently defined Structural SIMilarity index measurement (SSIM) (see [15], Section III-B, pp. 603–605). It can be noticed that we obtain better results when we use uninorms that when we use other detectors considered in this work.

II. FUZZY MORPHOLOGICAL OPERATORS

We assume as known the basics facts on uninorms used in this work which, in any case, can be found in [16], [17], [18]. We will use the following notation: \mathcal{I} is an implication, \mathcal{C} a conjunctive, \mathcal{N} a strong negation, and finally A is a gray-scale image and B is a gray-scale structural element.

We recall the definitions of fuzzy morphological operators following the ideas of De Baets in [5]. The method consists in fuzzify the logical operations, i.e. the Boolean conjunction and the Boolean implication, to obtain fuzzy operators. An n -dimensional gray-scale image is modeled as an $\mathbb{R}^n \rightarrow [0, 1]$ function. The values of an image must be in $[0, 1]$ in order to consider it as a fuzzy set. Then, we will proceed to explain this method from the following definitions and propositions.

Definition 2.1: The *fuzzy dilation* $D_{\mathcal{C}}(A, B)$ and *fuzzy erosion* $E_{\mathcal{I}}(A, B)$ of A by B are the gray-scale images

defined by

$$D_C(A, B)(y) = \sup_x \mathcal{C}(B(x - y), A(x)) \quad (1)$$

$$E_{\mathcal{I}}(A, B)(y) = \inf_x \mathcal{I}(B(x - y), A(x)). \quad (2)$$

Note that the reflection of a gray-scale image B denoted by $-B$, and defined by $-B(y) = B(-y)$, for all $y \in \mathbb{R}^n$. Given two images B_1, B_2 , we will say that $B_1 \subseteq B_2$ when $B_1(y) \leq B_2(y)$ for all $y \in \mathbb{R}^n$.

Definition 2.2: The *fuzzy closing* $C_{C, \mathcal{I}}(A, B)$ and *fuzzy opening* $O_{C, \mathcal{I}}(A, B)$ of A by B are the gray-scale images defined by

$$C_{C, \mathcal{I}}(A, B)(y) = E_{\mathcal{I}}(D_C(A, B), -B)(y) \quad (3)$$

$$O_{C, \mathcal{I}}(A, B)(y) = D_C(E_{\mathcal{I}}(A, B), -B)(y). \quad (4)$$

The conjunctors and implications used in this paper are two types of left-continuous conjunctive uninorms and their residual implications. Specifically these two types of uninorms are the following.

- The representable uninorms: Let $e \in]0, 1[$ and let $h : [0, 1] \rightarrow [-\infty, \infty]$ be a strictly increasing, continuous function with $h(0) = -\infty$, $h(e) = 0$ and $h(1) = +\infty$. Then $U_h(x, y) =$

$$\begin{cases} h^{-1}(h(x) + h(y)), & \text{if } (x, y) \notin \{(1, 0), (0, 1)\}, \\ 0, & \text{in other case,} \end{cases}$$

is a conjunctive representable uninorm with neutral element e , see [17], and its residual implication \mathcal{I}_{U_h} is given by $\mathcal{I}_{U_h}(x, y) =$

$$\begin{cases} h^{-1}(h(x) - h(y)), & \text{if } (x, y) \notin \{(0, 0), (1, 1)\}, \\ 1, & \text{in other case.} \end{cases}$$

Moreover, U_h satisfies self duality (except at the points (0,1) and (1,0) with respect to the strong negation $\mathcal{N}(x) = h^{-1}(-h(x))$, see [16].

- A specific type of idempotent uninorms: Let \mathcal{N} be a strong negation. The function given by

$$U^{\mathcal{N}}(x, y) = \begin{cases} \min(x, y), & \text{if } y \leq \mathcal{N}(x), \\ \max(x, y), & \text{in other case,} \end{cases}$$

is a conjunctive idempotent uninorm. Its residual implication is given by (see [18])

$$\mathcal{I}_{U^{\mathcal{N}}}(x, y) = \begin{cases} \min(\mathcal{N}(x), y), & \text{if } y < (x), \\ \max(\mathcal{N}(x), y), & \text{if } y \geq (x). \end{cases}$$

These two types of left-continuous conjunctive uninorms guarantee most of the good algebraic and morphological properties associated with the morphological operators obtained from them ([11]). Among these properties, we highlight those described below. In all properties, U is a left-continuous conjunctive uninorm with neutral element $e \in]0, 1[$, \mathcal{I}_U its residual implication, A is a gray-level image and B a gray-scale structural element.

- The fuzzy dilation D_U is increasing in both arguments, the fuzzy erosion $E_{\mathcal{I}}$ is increasing in their first argument and decreasing in their second one, the fuzzy closing C_{U, \mathcal{I}_U} and the fuzzy opening O_{U, \mathcal{I}_U} are both increasing in their first argument.
- If $B(0) = e$ the fuzzy dilation is extensive and the fuzzy erosion is anti-extensive $E_{\mathcal{I}_U}(A, B) \subseteq A \subseteq D_U(A, B)$. The fuzzy closing is extensive and the fuzzy opening is anti-extensive: $O_{U, \mathcal{I}_U}(A, B) \subseteq A \subseteq C_{U, \mathcal{I}_U}(A, B)$. Moreover, the fuzzy closing and the fuzzy opening are idempotent, i.e.: $C_{U, \mathcal{I}_U}(C_{U, \mathcal{I}_U}(A, B), B) = C_{U, \mathcal{I}_U}(A, B)$, and $O_{U, \mathcal{I}_U}(O_{U, \mathcal{I}_U}(A, B), B) = O_{U, \mathcal{I}_U}(A, B)$.
- If $B(0) = e$, then $E_{\mathcal{I}_U}(A, B) \subseteq O_{U, \mathcal{I}_U}(A, B) \subseteq A \subseteq C_{U, \mathcal{I}_U}(A, B) \subseteq D_U(A, B)$.
- For the two previous conjunctive uninorms of type U_h and $U^{\mathcal{N}}$, the duality between fuzzy morphological operators is guaranteed.

III. THE PROPOSED EDGE DETECTOR ALGORITHM

The main goal of this work is to develop an algorithm which can detect and preserve, in presence of noise, edge features in the low-contrast regions of medical images. In this work, we make use of a residual operator from fuzzy opening and closing operations in order to detect edge images and, at the same time, denoise the image. Recall that a residual operator of two morphological operations or transformations is their difference. In previous works, [11] and [10], we present the performance of fuzzy gradients and top-hat transformations based on uninorms in order to detect edges in natural images. In these works the displayed experiments show that the uninorms outperform the results obtained using t-norms and the classical umbra approach.

From the operation properties of the fuzzy morphology based on uninorms, it is satisfied that

$$O_{U, \mathcal{I}_U}(C_{U, \mathcal{I}_U}(A, B), B) \subseteq C_{U, \mathcal{I}_U}(A, B).$$

Let B be such that $B(0) = e$ and consider $F = O_{U, \mathcal{I}_U}(C_{U, \mathcal{I}_U}(A, B), B)$. So we have (see [11])

$$\begin{aligned} E_{\mathcal{I}_U}(C_{U, \mathcal{I}_U}(F, B), B) &\subseteq C_{U, \mathcal{I}_U}(F, B) \\ &\subseteq D_U(C_{U, \mathcal{I}_U}(F, B), B). \end{aligned}$$

Then we can compute the next residual operator

$$\delta_{U, \mathcal{I}_U}^{1+}(A, B) = D_U(C_{U, \mathcal{I}_U}(F, B), B) \setminus C_{U, \mathcal{I}_U}(F, B). \quad (5)$$

In equation (5), the so called *alternate filters*, alternate composition of opening and closing, are involved. These alternate filters are used to remove and to smooth noise in [10]. So, the proposed algorithm is the following: Firstly, we preprocess the image by an alternate filter in order to filter the noise and smooth the image, and then we apply a Beucher gradient by dilation. Once the residual image (5) is obtained, a global threshold experimentally obtained is then applied to transform the edge image into a binary image.

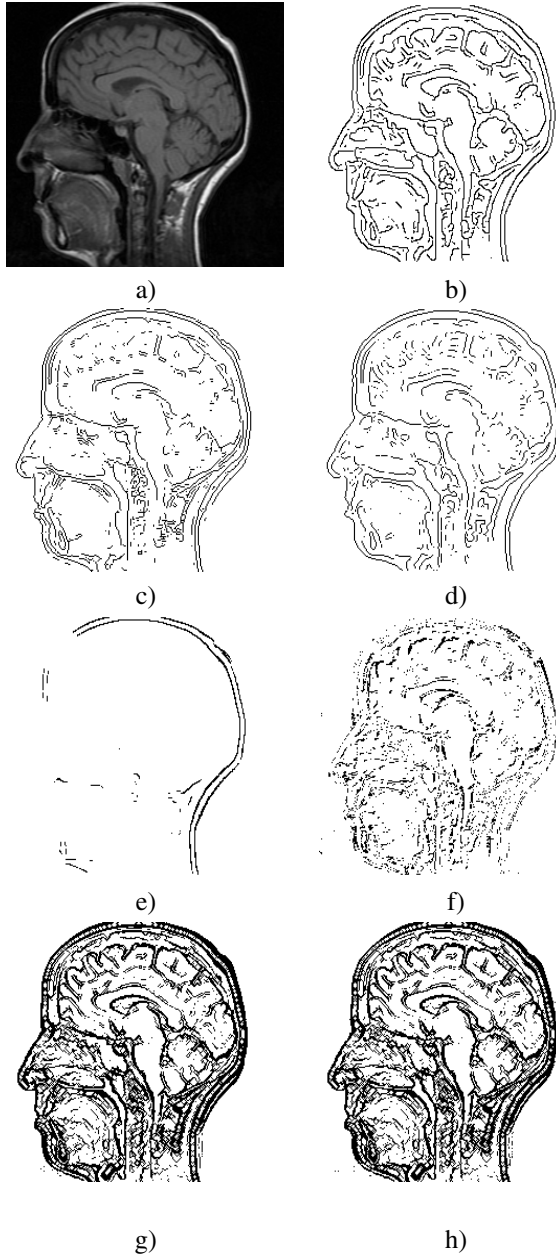


Figure 1. a) Original MRI image. b), c) and d) edge detection obtained by Canny, Prewitt and LoG edge detectors, respectively. e) using the proposed algorithm with Łukasiewicz t-norm and umbra approach, respectively. g), h) results obtained by the proposed approach using a representable and idempotent uninorm, respectively.

The previous filtering of the image allows us to minimize the effect of the noise on the image without altering or slightly altering the outer edge of the regions that compose the image and maintaining the edge features of the image. To binarize the obtained image in (5), a value threshold between 0.85 and 0.98 of the maximum value of the histogram is taken. In the next section we present some experimental results obtained using the previous algorithm.

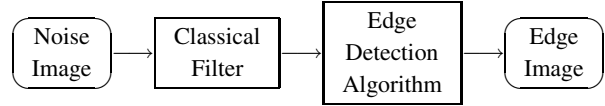


Figure 2. Block diagram for edge detection.

IV. EXPERIMENTAL RESULTS AND ANALYSIS

In the following experiments, the idempotent uninorm $U^{\mathcal{N}}$ with $\mathcal{N}(x) = 1 - x$ and the representable uninorm U_h with $h(x) = \ln\left(\frac{x}{1-x}\right)$ have been used. The obtained results are compared with the Łukasiewicz t-norm and the classic development based on *umbra approach* (see [7]). In particular, the structural element used by the morphological operators is given by a 3×3 matrix:

$$\begin{pmatrix} 0 & 1 & 0 \\ 1 & 1 & 1 \\ 0 & 1 & 0 \end{pmatrix} \cdot e \quad (6)$$

where e is the neutral element of the uninorm.

The performance of the proposed fuzzy mathematical morphology based on edge detection algorithm is evaluated in this section, and experimental results compared with other existing methods are also presented. The method has been applied to medical images and salt and pepper noise corrupted medical images. The noise in the images has been added using the standard functions of Matlab R2008a. Also, the edge images processed by the Canny, Prewitt, LoG (Laplacian of Gaussian operator), Zero-Cross and Roberts edge detectors have been obtained using default parameters of Matlab. Except in Fig. 1.c) where we have used a sensitivity threshold for the Prewitt method equal to 0.05 because, in this case, we got an almost empty edge image using the default setting. In all cases, various sets of parameters have been tested and only those providing more adequate results are shown in the figures.

The MRI head image shown in Fig. 1.a) of size 256×228 contain dark regions and many features of brain wrinkles and head cavities. The contrast in these dark regions is so low that edge features in these regions are very difficult to detect. Canny [19] and many others establish the unavoidable trade-off between localization and signal strength. The Canny, Prewitt, LoG edge detectors are applied to the image and the experimental results are displayed in Fig. 1.b)-d). The results obtained with the proposed algorithm using the Łukasiewicz t-norm as conjunction and its residual implication and using the classical umbra approach are displayed in Fig. 1.e)-f). It can be seen that the performance of the proposed edge detector algorithm using uninorms (Fig. 1.g-h)) is better than those of the previous ones. Using uninorms and the proposed algorithm, many thin features in the MRI head image are detected and have a strong intensity. In [11] we can see as the edge images obtained by a pure morphological approach (morphological gradient) produce a good edge detection

performance, but many really thin edges are still unable to be detected.

In the following experiments, noise type salt and pepper was added to the test images in order to study the robustness of the proposed algorithm. To remove noise in the image, a classical filter of $n \times n$ mask was applied to the noisy image before applying a classical edge detector algorithm. In particular a median filter with $n = 3$ was applied to remove salt and pepper noise and a Wiener filter with $n = 5$ was applied in presence of Gaussian noise. The block

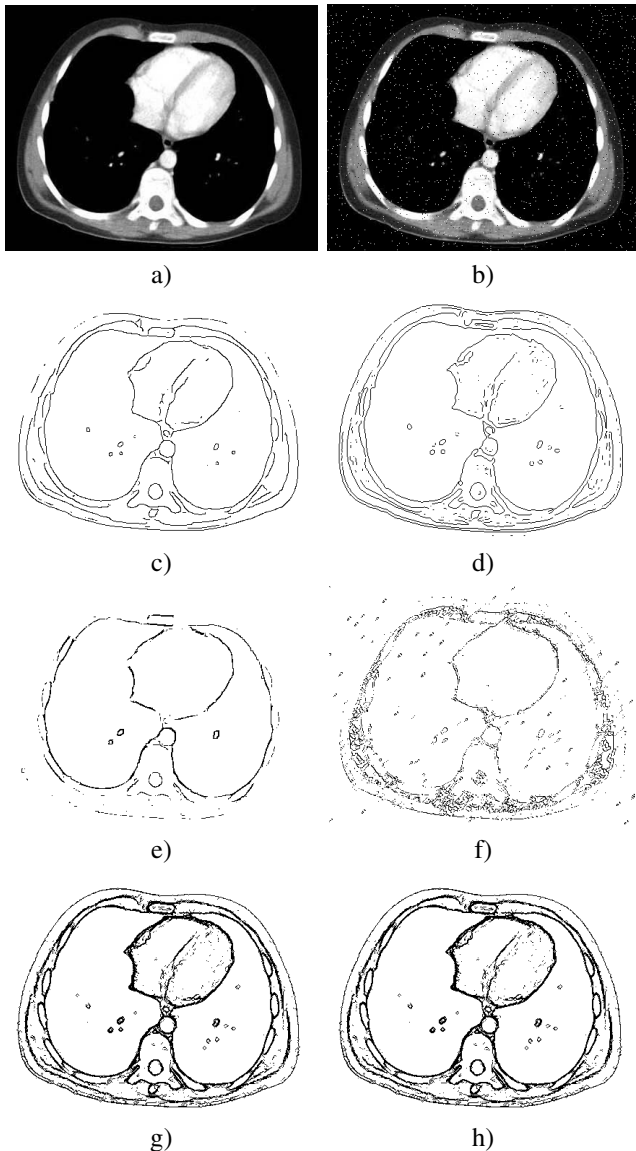


Figure 3. a) Original lungs CT image. b) corrupted with 0.02 salt and pepper noise. c), d) results by Canny and zero-cross edge detectors, respectively. e), f) results obtained by the proposed algorithm using the Łukasiewicz t-norm and umbra approach, respectively. g), h) results obtained by the proposed algorithm using a representable and an idempotent uninorm, respectively.

diagram of the process is illustrated in Fig. 2. With this set of experiments we show that the proposed edge detection algorithm can adequately extract edge features even when the image is noisy.

The original lungs CT image of size 430×338 displayed in Fig. 3.a) contains many interesting features. A salt and pepper noise function with parameter 0.02 was added to the image (Fig. 3.b)). In this case, the Canny and zero-cross were also applied to the image after a median filter was used to remove noise. The proposed algorithm using representable and idempotent uninorms can successfully extract the boundaries of the lungs and the main edge features of the image. Compare with the so one obtained using t-norms and the umbra approach. Note that, the Canny edge detector fails to detect the outer edge of body, and the two classical edge detectors fail to separate the boundaries of the lungs, showing some gaps in the obtained boundary. Something similar happens with the detected edges of osseous structures.

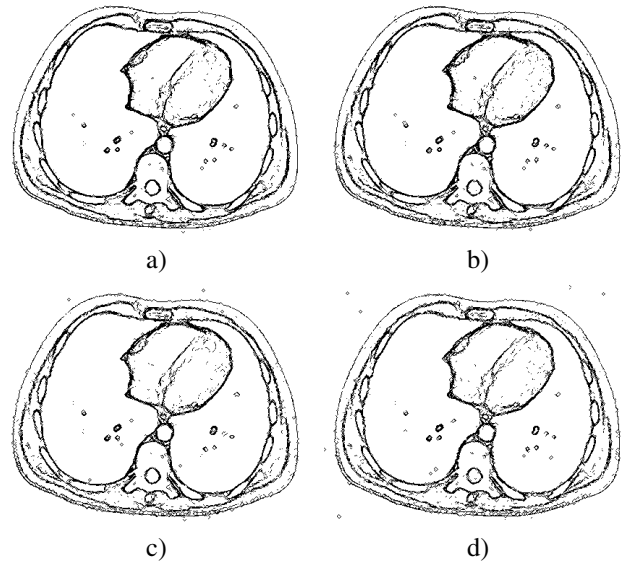


Figure 4. From left to right and from top to bottom, results obtained by the proposed algorithm using the same idempotent uninorm and structural element than in Fig. 3.h), when we corrupted the original image with 0.04, 0.06, 0.08 and 0.1 salt and pepper noise, respectively.

In Fig. 4 we display the results obtained by the proposed fuzzy edge detection algorithm when four different salt and pepper noise functions, of parameter 0.04, 0.06, 0.08 and 0.1 respectively, were added to the image shown in Fig. 3.a). Our goal is to study the performance of the proposed algorithm when we increase the amount of noise present in the image. The results obtained with the proposed algorithm are shown in Fig. 4.a-d). Comparing these results with those shown in Fig. 3.h), we can see as the edges image are little affected with the increase of noise and many features remain detected.

Table I
MSE, SNR AND SSIM FOR FILTERED IMAGES OF FIG. 3

Filter type	MSE	SNR	SSIM
Corrupted Img.	578.826	11.0088	0.96108
Umbra App.	1228.39	7.74087	0.920127
Luk. t-norm	148.08	16.9293	0.989052
Idempotent	26.6825	24.372	0.998137
Representable	26.6826	24.378	0.998139

A number of different objective measures can be utilized to evaluate the previous filtering step in our fuzzy approach providing a quantitative evaluation of the filtering results. Among them, the MSE, the SNR, and the SSIM (see [15]). Let O_1 and F_2 be two images of dimensions $M \times N$. We suppose that O_1 is the original noise-free image and F_2 is the restored image for which some filter has been applied. The MSE, SNR, and SSIM values defined in Eqs. 7, 8 and 9 are used to evaluate the filtering performance.

$$MSE(F_2, O_1) = \frac{1}{MN} \sum_{i=1}^M \sum_{j=1}^N (O_1(i, j) - F_2(i, j))^2. \quad (7)$$

$$SNR(F_2, O_1) = 10 \cdot \log_{10} \left(\frac{\sigma_1^2}{MSE} \right), \quad (8)$$

where σ_1^2 is the variance of the original image O_1 ,

$$SSIM(F_2, O_1) = \frac{(2\mu_1\mu_2 + C_1)}{(\mu_1^2 + \mu_2^2 + C_1)} \cdot \frac{(2\sigma_{12} + C_2)}{(\sigma_1^2 + \sigma_2^2 + C_2)}, \quad (9)$$

where μ_k , $k = 1, 2$ is the mean of the image O_1 and F_2 respectively, σ_k^2 is the variance of each image, σ_{12} is the covariance between the two images, $C_1 = (0.01 \cdot 255)^2$ and $C_2 = (0.03 \cdot 255)^2$ (see [15] for details). Recently, SSIM was introduced under the assumption that human visual perception is highly adapted for extracting structural information from a scene. The SSIM is an alternative complementary framework for quality assessment based on the degradation of structural information. Smaller values of MSE and larger values of both SNR and SSIM ($0 \leq SSIM \leq 1$) are indicators of better capabilities for noise reduction and image recovery.

The values of these measures between the original image and filtered image $C_{U, \mathcal{I}_U}(F, B)$, where $F = O_{U, \mathcal{I}_U}(C_{U, \mathcal{I}_U}(A, B), B)$, are depicted in Table I. It can be noticed that when we use uninorms the measures are improved with respect to the other cases. Table II shows the values of these measures in function of the amount of noise added to the original image in the experiments of Fig. 4. Notice that, when the noise increase, the values of the measures remain acceptable and SSIM values are still higher than 0.99.

Finally, Fig. 5 shows an experiment in which the original image is corrupted with Gaussian noise of parameter 0.005. A Wiener filter is applied, because it works better than the median filter in presence of Gaussian noise, previously to the

Table II
MSE, SNR AND SSIM FOR FILTERED IMAGES OF EXPERIMENTS DISPLAYED IN FIG. 4.

Noise Parameter	MSE	SNR	SSIM
0.02	26.6825	24.372	0.998137
0.04	41.1434	22.4912	0.9971357
0.06	50.7033	21.5839	0.996468
0.08	70.2527	20.1676	0.995104
0.1	102.487	18.5275	0.992877

classical edge detection method. In this case the structural element used by the morphological operators is a 5×5 matrix given by

$$\begin{pmatrix} 0 & 0 & 1 & 0 & 0 \\ 0 & 1 & 1 & 1 & 0 \\ 1 & 1 & 1 & 1 & 1 \\ 0 & 1 & 1 & 1 & 0 \\ 0 & 0 & 1 & 0 & 0 \end{pmatrix} \cdot e \quad (10)$$

where e is the neutral element of the uninorm. It can be seen how the edge images obtained using the fuzzy proposed approach produce a good edge detection performance. Observe that the classical approaches fail to detect some main edge features of the image.

V. CONCLUSIONS AND FUTURE WORK

In this work, an edge detection algorithm based on the fuzzy morphology using uninorms, derived as a residual operator from the basic morphological operations, has been proposed. Such algorithm is able to detect the features in low contrast regions, and preserve them as well as other apparent edges. To evaluate the performance of the algorithm, comparison experiments with other well known approaches were carried out. The results indicate that the proposed algorithm is robust against noisy images. Experimental results show that it outperforms other edge detection methods in detecting detailed edges features and thin edge features, in the displayed medical images. Moreover, these edges can be preserved even though the image is corrupted by noise. Future work consists on one hand, in the study of the behaviour of the algorithm when we increase the Gaussian noise and, on the other hand in the selection of the size, shape, direction of the structuring element adapted to the edge features of the image and how

ACKNOWLEDGMENT

This work has been supported by the Government Spanish Grant MTM2006-05540, MTM2009-10320 and TIN2007-67993, with FEDER support.

REFERENCES

- [1] W. K. Pratt, *Digital Image Processing*, 4th ed. Wiley-Interscience, February 2007.

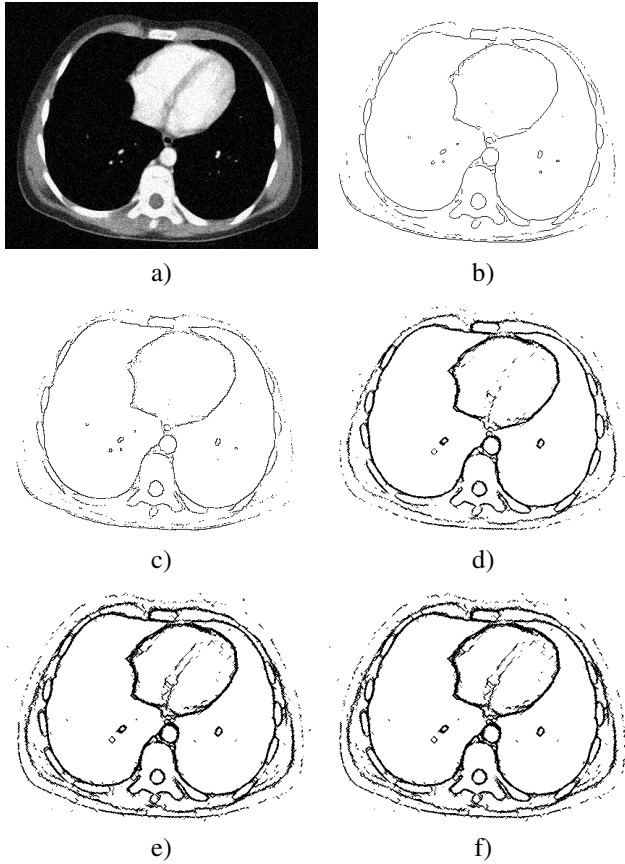


Figure 5. a) Image corrupted with 0.005 Gaussian noise. b), c) edge images obtained using Prewitt and Roberts edge detectors, respectively. d), e) and f) results obtained by the proposed algorithm using the Lukasiwicz t-norm, a representable and an idempotent uninorm, respectively.

- [2] H. Bustince, E. Barrenechea, M. Pagola, and J. Fernandez, "Interval-valued fuzzy sets constructed from matrices: Application to edge detection," *Fuzzy Sets Syst.*, vol. 160, no. 13, pp. 1819–1840, 2009.
- [3] J. Serra, *Image analysis and mathematical morphology, vols. 1, 2*. London: Academic Press, 1982,1988.
- [4] I. Bloch and H. Maître, "Fuzzy mathematical morphologies: a comparative study," *Pattern Recognition*, vol. 28, pp. 1341–1387, 1995.
- [5] B. De Baets, "Fuzzy morphology: A logical approach," in *Uncertainty Analysis in Engineering and Science: Fuzzy Logic, Statistics, and Neural Network Approach*, B. M. Ayyub and M. M. Gupta, Eds. Norwell: Kluwer Academic Publishers, 1997, pp. 53–68.
- [6] B. De Baets, E. Kerre, and M. Gupta, "The fundamentals of fuzzy mathematical morfologies part i: basics concepts," *International Journal of General Systems*, vol. 23, pp. 155–171, 1995.
- [7] M. Nachtegaele and E. Kerre, "Classical and fuzzy approaches towards mathematical morphology," in *Fuzzy techniques in image processing*, ser. Studies in Fuzziness and Soft Computing, E. E. Kerre and M. Nachtegaele, Eds. New York: Physica-Verlag, 2000, no. 52, ch. 1, pp. 3–57.
- [8] B. De Baets, N. Kwasnikowska, and E. Kerre, "Fuzzy morphology based on uninorms," in *Proceedings of the seventh IFSA World Congress, Prague, 1997*, pp. 215–220.
- [9] M. González-Hidalgo, A. Mir-Torres, and D. Ruiz-Aguilera, "A robust edge detection algorithm based on a fuzzy mathematical morphology using uninorms (ϕ MM-U morphology)," in *VipIMAGE 09, accepted*.
- [10] M. González-Hidalgo, A. Mir-Torres, D. Ruiz-Aguilera, and J. Torrens, "Image analysis applications of morphological operators based on uninorms," in *IFSA-EUSFLAT 09*, pp. 630–635.
- [11] —, "Edge-images using a uninorm-based fuzzy mathematical morphology: Opening and closing," in *Advances in Computational Vision and Medical Image Processing*, ser. Computational Methods in Applied Sciences, J. Tavares and N. Jorge, Eds. Netherlands: Springer, 2009, no. 13, ch. 8, pp. 137–157.
- [12] J.-A. Jiang, C.-L. Chuang, Y.-L. Lu, and C.-S. Fahn, "Mathematical-morphology-based edge detectors for detection of thin edges in low-contrast regions," *IET Image Processing*, vol. 1, no. 3, pp. 269–277, 2007.
- [13] Y. Xu, J. Zhao, and Y. Jiao, "Noisy image edge detection based on multi-scale and multi-structuring element order morphology transformation," in *CISP '08, Vol. 3*. IEEE Computer Society, 2008, pp. 379–383.
- [14] Z. Yu-qian, G. Wei-hua, C. Zhen-cheng, T. Jing-tian, and L. Ling-yun, "Medical images edge detection based on mathematical morphology," in *Proceedings of the 2005 IEEE Engineering in Medicine and Biology 27th Annual Conference, Shanghai, China, 2005*, pp. 6492–6495.
- [15] Z. Wang, A. C. Bovik, H. R. Sheikh, and E. P. Simoncelli, "Image quality assessment: From error visibility to structural similarity," *IEEE Transactions on Image Processing*, vol. 13, no. 4, pp. 600–612, 2004.
- [16] B. De Baets and J. Fodor, "Residual operators of uninorms," *Soft Computing*, vol. 3, pp. 89–100, 1999.
- [17] J. Fodor, R. Yager, and A. Rybalov, "Structure of uninorms," *Int. J. Uncertainty, Fuzziness, Knowledge-Based Systems*, vol. 5, pp. 411–427, 1997.
- [18] D. Ruiz-Aguilera and J. Torrens, "Residual implications and co-implications from idempotent uninorms," *Kybernetika*, vol. 40, pp. 21–38, 2004.
- [19] J. Canny, "A computational approach to edge detection," *IEEE Trans. Pattern Anal. Mach. Intell.*, vol. 8, no. 6, pp. 679–698, November 1986.